

We are IntechOpen, the world's leading publisher of Open Access books Built by scientists, for scientists

6,900

Open access books available

185,000

International authors and editors

200M

Downloads

Our authors are among the

154

Countries delivered to

TOP 1%

most cited scientists

12.2%

Contributors from top 500 universities



WEB OF SCIENCE™

Selection of our books indexed in the Book Citation Index
in Web of Science™ Core Collection (BKCI)

Interested in publishing with us?
Contact book.department@intechopen.com

Numbers displayed above are based on latest data collected.
For more information visit www.intechopen.com



The Coupled Magnetic Field Effects on the Microstructure Evolution and Magnetic Properties of As-Deposited and Post-Annealed Nano-Scaled Co-Based Films — Part I

Donggang Li, Qiang Wang, Agnieszka Franczak, Alexandra Levesque and Jean-Paul Chopart

Additional information is available at the end of the chapter

<http://dx.doi.org/10.5772/61270>

Abstract

Superimposed external magnetic fields during electrodeposition process offers the possibility to tailor microstructure and properties of the obtained films in a very efficient, contactless, and easily controllable way, what is caused by so-called magnetohydrodynamic (MHD) effect. On the other hand, the nonequilibrium state of as-electrodeposited nanocrystalline films provides a strong thermodynamic potential for microstructural transformation. This means that the benefit effect of magneto-electrodeposition on a nanocrystalline film can be completely consumed by a thermal exposure at relatively low temperature. Magnetic field annealing has been confirmed to be useful for tailoring the microstructure of as-deposited nanocrystalline films for their widespread uses.

The particular interest of this book Chapter “Growth of Co-based magnetic thin films by magnetic fields (MF) assisted electrodeposition and heat treatment” is the finding that the microstructure and magnetic properties of nanocrystalline Co-based alloys and oxides like CoX (X= Cu, Ni, NiP, FeO) are improved by imposition of MF during elaboration process or post-annealing process. According to the previous study, the targeted scientific activities pay more attention to develop alloys and oxides in nano-scale using pulsed electrodeposition assisted by high magnetic field (HMF). (Note: Since the instantaneous current density during pulse electrodeposition is higher than that during direct current plating, the microstructure of the nano-scale electrodeposits can be more easily controlled by perturbing the desorption/adsorption processes occurring in the pulse electrodeposition process).

During the experiment, high magnetic field is an in-situ method for the control of electrodeposition process. The obtained material is then annealed or oxidized after

elaboration under HMF. Comparative studies are performed concerning the electrodeposition process in a high magnetic field, by changing the magnetic field parameters such as magnetic flux density, direction, gradient. Then, we will investigate the evolution of the microstructure induced by magnetic field, and the control of crystal orientation, crystal size, and its distribution by a HMF. By comparing the microstructure and magnetic properties of the film with and without a HMF, we can find optimum magnetic field parameters for the control of the growth of nanocrystalline Co-based magnetic film. The functionality of materials could then be improved by both processes under HMF: electrodeposition and annealing.

Keywords: coupled magnetic field effects, microstructure evolution, nano-scaled Co-based films

1. High magnetic field annealing dependent on the morphology and microstructure of electrodeposited Co/Ni bilayered films

1.1. Introduction

Electrodeposited nanocrystalline magnetic films have received considerable interest in the fields of data storage devices and microelectromechanical systems (MEMS) [1], since the microstructure of the film can be easily controlled on a large scale during the electrochemical processing in comparison with a physical vapor deposition. It is well known that the physical properties of the electrodeposits strongly depend on morphology and microstructure, as reported in recent papers [2-3]. Numerous studies have been devoted to improve surface morphology and microstructure, i.e., reducing the grain size and the roughness, by magneto-hydrodynamic effect (MHD), which is induced by superimposing an external magnetic field [4-6] during the electrodeposition process. However, the nonequilibrium state of as-electrodeposited nanocrystalline layers provides a strong thermodynamic potential for microstructural transformation. This means that the benefit effect of magneto-electrodeposition on a nanocrystalline film can be completely consumed by a thermal exposure at relatively low temperature [7]. Magnetic field annealing has been confirmed to be useful for tailoring the microstructure of as-deposited nanocrystalline films for their widespread uses [8]. Markou et al. [9] obtained a high-degree (001) texture in $L1_0$ CoPt films by annealing Co/Pt bilayers in a perpendicular magnetic field of 1 kOe. The advancement of superconducting technology has opened unique aspects for heat treatment in a high magnetic field. Up to date, few applications of high magnetic field (over 10 T) during annealing process [10] proved it to be a promising method to control the preferential crystallographic orientation of the deposited magnetic film. Though there is no doubt that high magnetic field annealing plays an important role on grain growth, inter-diffusion [11-13], and recrystallization processes, which in turn will influence the microstructural variation of nanocrystalline film, the dependences of grain shape, grain size, roughness, and texture of electrodeposited films on the magnetic field parameters during post-annealing are still unclear. In this study, we investigate the effect of post-high magnetic

field annealing up to 12 T on Co/Ni bilayered film obtained by electrodeposition assisted with or without a 0.5 T magnetic field.

1.2. Experimental

Nanocrystalline bilayered films were electrodeposited on ITO (1000 nm thickness)/ glass (1 cm²) with the structure of ITO glass/Ni/Co from two cells step by step. One cell contained the electrolyte of nickel sulfate 0.6 M, boric acid 0.4 M, and pH was adjusted to 2.7 at 30°C. The electrolyte in the other cell consisted of cobalt sulfate 0.6 M, boric acid 0.4 M, at 50°C, pH = 4.7. The counter electrode was a rectangular Pt plate of 1×2cm, placed parallel to the working electrode. Chronopotentiometry method with a current density of 10 mA /cm² was performed for 6 min in Ni²⁺ cell, and 4 min in Co²⁺ cell, respectively. A water-cooled electromagnet was used to produce a magnetic field of 0.5 T. The magnetic field was superimposed parallel to the working electrode during the electrodeposition processing of Co film. Two series of electrodeposits were denoted, 0 T-B_{ed} and 0.5 T-B_{ed}.

The two series of as-deposited films were heat-treated at 673 K for 4 h under a protective atmosphere of high-purity argon in a vertical furnace, which was placed inside a superconducting magnet of up to 12 T, and then cooled down to room temperature. The direction of the high magnetic fields was vertically upward, in perpendicular to the horizontally placed films, while the strengths of the magnetic fields were 0, 6, and 12T, respectively.

The surfacial morphology of the Co/Ni films was observed by using a field emission scanning electronic microscopy (FE-SEM, SUPRA 35) made in Japan with high magnification times. The topography and the roughness were investigated by the AFM (NTEGRA AURA, NT-MDT, Russia). Each sample was measured in areas of 10μm×10μm for three times at different positions of the film to obtain the average grain size and roughness of the surface. For the characterization of the films microstructure, Grazing Incidence X-Ray Diffraction (GI-XRD, Ultima IV, Japan) measurements were performed using the Cu Kα radiation (40 kV, 40 mA, λ=1.54Å). X-ray photoelectron spectroscopy (XPS) measurement (ESCALAB250, Thermo VG Company, USA) was done to analyze the distribution of Co and Ni along the cross-section of the samples, by which the thickness of Co layer can also be estimated as about 1200 nm.

1.3. Results and discussion

The FE-SEM images in Figure 1 show the surface morphology of annealed Co/Ni films under high magnetic fields of 0, 6, 12 T. By comparing the Figure 1(a1-a3) and Figure 1 (b2-b3), it can be seen that the application of high magnetic field annealing played a similar role on the morphological evolution in both series: 0 T-B_{ed} and 0.5 T-B_{ed}, although there is a obvious difference between the two series, which were annealed at the same 6 T magnetic field condition. It is generally considered that the effects of a weak magnetic field (B_{ed}) on the morphology of electrodeposits were almost fully consumed by an annealing process for a long time. The films after post-annealed under 0 T magnetic field present a blurred irregular grain shape with a mass of velour-like deposits on the grain boundary. With the increase of the applied magnetic field, not only the grain shape and grain boundary become clear to form

polyhedral grains but also the grain size decreases with the disappearance of the velour-like deposits.

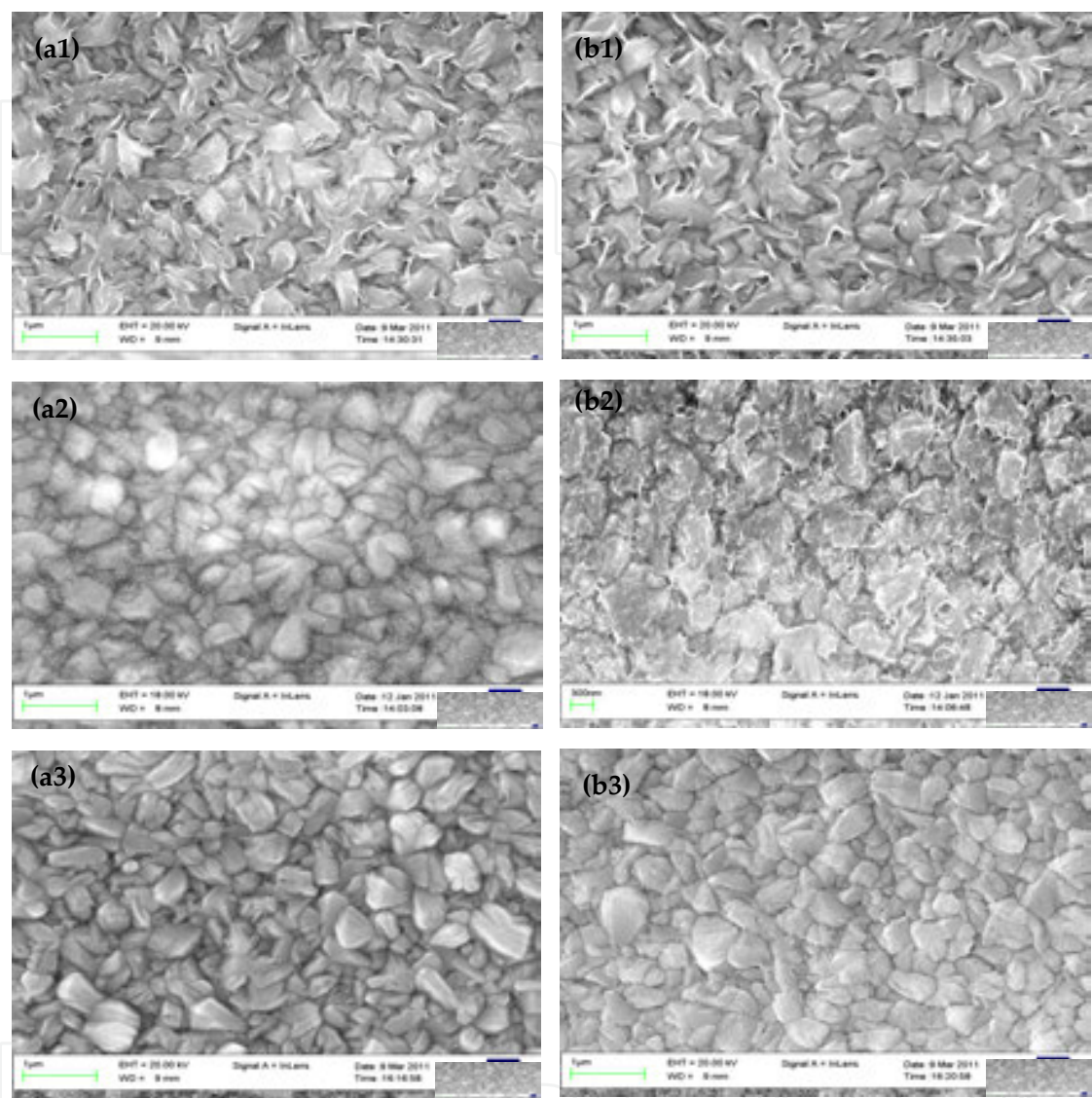


Figure 1. FE-SEM images of 0 T-B_{ed} series Co/Ni film annealed under different magnetic fields (a1) 0 T, (a2) 6 T, (a3) 12 T, and (b1) 0 T, (b2) 6 T, (b3) 12 T. [48]

As it is well known, for magnetic and paramagnetic materials, magnetic field will induce a pulling force due to the magnetization [14–15], which force is favored for the separation of magnetization. In the present work, an infrared for the separation of grain boundary during the magnetic field annealing results in the decrease of diffusion activation energy, which will improve the diffusion of the congregated deposits on the grain boundary. This is a possible reason for the grain boundary becoming clear after post-magnetic field annealing. Another most likely reason for the disappearance of velour-like product, which is estimated to be Co-oxides formed at the grain boundaries, is that the application of high magnetic fields during annealing process is favorable for the reduction of oxides, but the mechanism needs further investigation.

On the other hand, we should also take into account the effect of the magnetic field annealing on recrystallization process and grain boundary migration (GBM) in the films. If magnetic field annealing plays a retarded effect on the recrystallization process as reported by Refs. [16–17] or beneficial effects on GBM due to magnetic ordering as reported by Molodov et al [18], the grain size of the film after post-magnetic annealing should be larger than the case

On the other hand, we should also take into account the effect of the magnetic field annealing on recrystallization process and grain boundary migration (GBM) in the films. If magnetic field annealing plays a retarded effect on the recrystallization process as reported by Refs. [16-17] or beneficial effects on GBM due to magnetic ordering as reported by Molodov et al [18], the grain size of the film after post-magnetic annealing should be larger than the case of annealing without a magnetic field. However, no such effects of magnetic annealing on the electrodeposited film were observed in our experiments, since we found that the grain size of the film annealed under a high magnetic field seemed smaller than that of the annealed film under a no-field condition.

In order to quantitatively analyze the effects of high magnetic fields on the roughness and the grain size of the bilayered film, AFM top view ($10 \times 10 \mu m^2$) and three-dimensional AFM image of the surface topography of nanocrystalline films annealed at different magnetic flux densities ($B_{\text{annealing}}$) are shown in Figure 2. The grain shape of the films is similar for the two series samples annealed under magnetic flux densities of 12 T, therefore we only provide the AFM images of 0.5 T- B_{ed} series here. After no-field annealed, there are some ellipsoidal grains imbedded in the spherical grain matrix as seen in Figure 2 (a). While annealing in a magnetic field of 12 T, most of the grains are spherical, even some grains connect with each other to form a chain-like structure (Figure 2 (c)).

To characterize the grain size and the surface roughness, the average values were calculated using standard software (Table 1). For 0 T- B_{ed} series, the application of 6 T magnetic field during annealing process does not affect the grain size, but leads to a decrease of surface roughness. The grain size of the films goes through minimum under the influence of a 12 T magnetic field annealing. On the other hand, in case of 0.5 T- B_{ed} series, 6 T magnetic field annealing is enough to decrease the average grain size of the film from 140 to 100 nm.

The same magnetic annealing conditions inducing different results between the two series indicate that the influence of a weak magnetic field on the electrodeposition process can be conserved in a certain extent after post-annealing process. As the alternation of grain size during magnetic field annealing is not in a general correlation with that of surface roughness, some researchers [19] also showed that a decrease of grain size was not necessarily corresponding to a decrease in the surface roughness.

According to the results in Table 1, AFM investigations show that smaller grains and lower roughness are formed during annealing in the presence of a magnetic field comparing with the case of annealing without magnetic field. This phenomenon originates from an accelerative effect of the high magnetic fields annealing on the inter-diffusion between Co and Ni films. The initial as-deposited Co film on the surface consists of 20-50 nm sized grains, which distributed nonuniform with a large number of agglomerate as shown in Figure 3. For a given set of annealing conditions, the nanocrystalline matrix consumed by grain growth, the mean grain size continues to increase. At the meantime, inter-diffusion behavior happens between the Co and the Ni films, which results in Co atoms diffuse into the Ni matrix to form Co-Ni alloy. The application of high magnetic fields during annealing process improved the inter-diffusion behavior according to the conclusions in Refs. [11] and [20]. The experimental

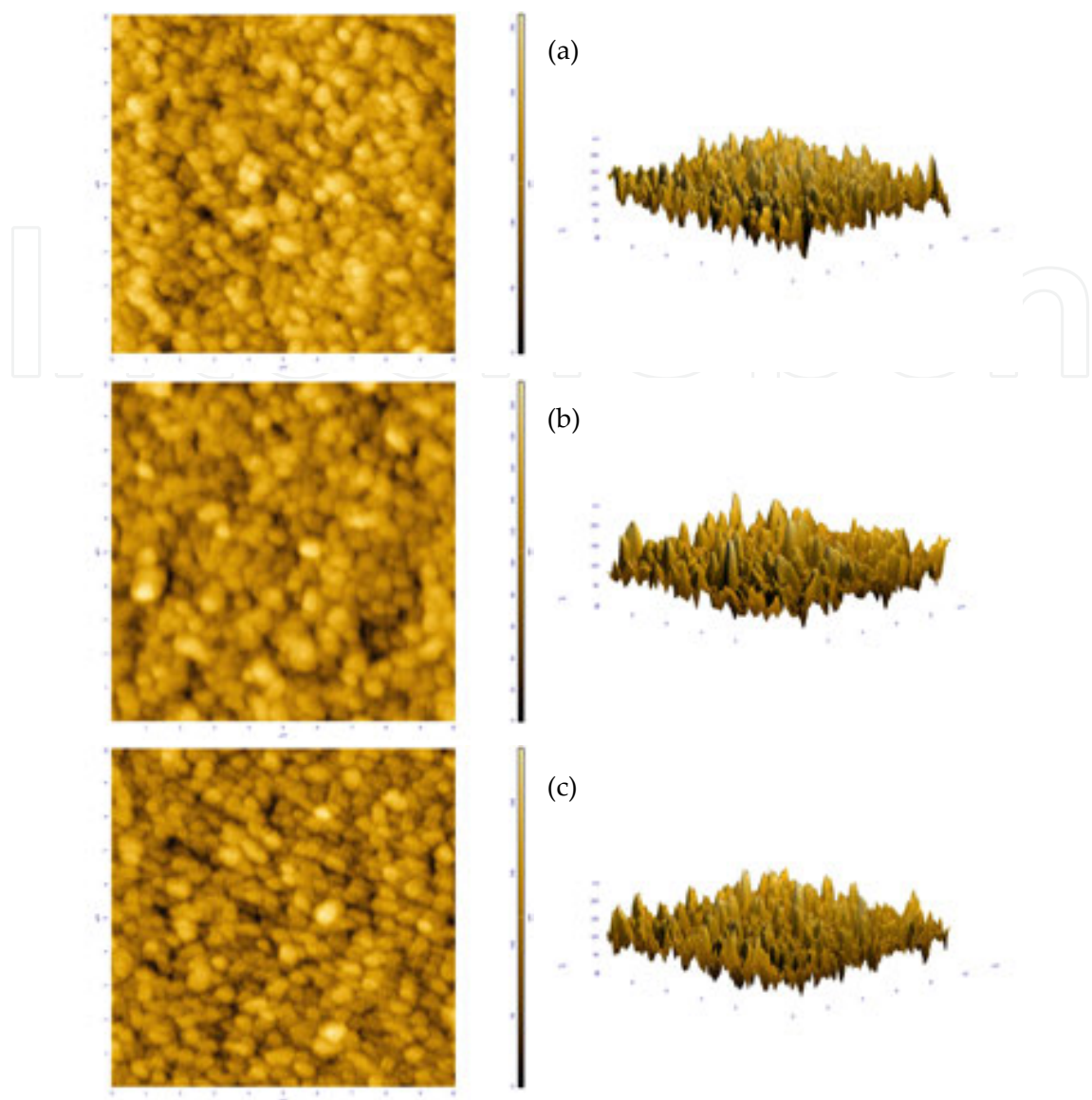


Figure 2. AFM images showing the morphology and roughness of 0.5 T-B_{ed} series Co/Ni films annealed under different magnetic fields (a) 0 T, (b) 6 T, (c) 12 T. [48]

Series	Series	B _{annealing}	Grain size (nm)		Roughness (nm)
			Grain size (nm)	Grain size (nm)	
0 T-B _{ed}	0 T-B _{ed}	0 T	127 ± 5	127 ± 5	29 ± 1.9
		6 T	128 ± 3	128 ± 3	23 ± 1.8
		12 T	114 ± 3	114 ± 3	25 ± 0.9
0.5 T-B _{ed}	0.5 T-B _{ed}	0 T	140 ± 6	140 ± 6	28 ± 1.5
		6 T	100 ± 3	100 ± 3	22 ± 1.2
		12 T	104 ± 4	104 ± 4	24 ± 1.6

Table 1. Dependence of the average grain size and the average roughness of the two series films on the magnetic flux density of the applied magnetic field annealing. [48]

The same magnetic annealing conditions inducing different results between the two series indicate that the influence of a weak magnetic field on the electrodeposition process can be conserved in a certain extent after post-annealing process. As the alternation of grain size during magnetic field annealing is not in a general correlation with that of surface roughness, some researchers [19] also showed that a decrease of grain size was not necessarily corresponding to a decrease in the surface roughness.

evidence of this improved inter-diffusion distance by magnetic field from 920 (0 T) to 1330 nm (12 T) was obtained by XPS analysis along the cross-section of the samples. Larger volume fraction of Co-Ni nanocrystalline alloy is formed, smaller is the mean grain size. It is attributed to the crystallographic texture of Co-Ni alloy in $\alpha(fcc)$ phase comparing with $\epsilon(hcp)$ -Co, which will be discussed in detail in the next section. Another possible explanation for the results in this study is the effect of field annealing on the magnetic domains. The magnetic domains tend to be directional ordering due to magnetization under magnetic annealing, which results in the decrease of the distance between domain walls, as in turn may be responsible for the smaller grain size.

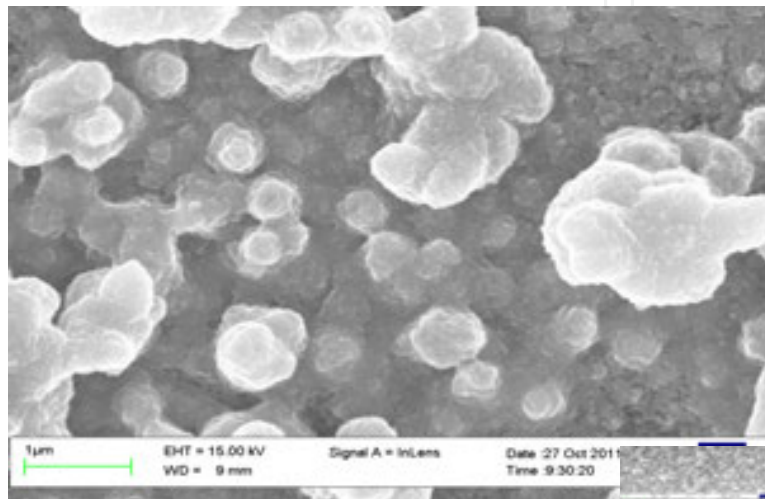


Figure 3. FE-SEM image of the as-deposited Co/Ni film (0 T- B_{ed} series) before annealing.[48]

Figure 4 presents XRD patterns for 0.5 T- B_{ed} series Co/Ni films in the post-magnetic annealing state with magnetic fields of 0, 6, and 12 T (Note: The 0 T- B_{ed} series annealed under a high magnetic field show similar XRD patterns as the 0.5 T- B_{ed} series). It can be seen that all the peaks of hcp-Co and fcc-Ni have been detected, but only one peak (220) of fcc-CoNi have been measured because of the alloying process. The diffraction peak (111) shifts to slightly higher diffraction angles in case of magnetic flux density of 6 T. One reason for the shift is most probably because of the internal stress. Some researchers [9] found the magnetic field annealing can change the internal stress state of films. This behavior can also be rationalized as another reason: more Co atoms are incorporated into the Ni lattice under the moderate magnetic field annealing resulting in a transition from Ni-like microstructural evolution to Co-like microstructural evolution [3].

Since the mean grain size D calculated by Scherrer's formula $D = \frac{k\lambda}{\beta \cos\theta}$ is in inverse ratio to β , where β is the full width at half maximum (FWHM) [21]. Here, we list the width and the position of the peaks in Table 2. It can be seen from the data that the width of peaks mostly increases with the increasing magnetic flux density. This also means that the grain size decreased with the magnetic flux density. The change of grain size D is in the same trend as the results obtained from AFM.

under the moderate magnetic field annealing resulting in a transition from Ni-like microstructural evolution to Co-like microstructural evolution [3].

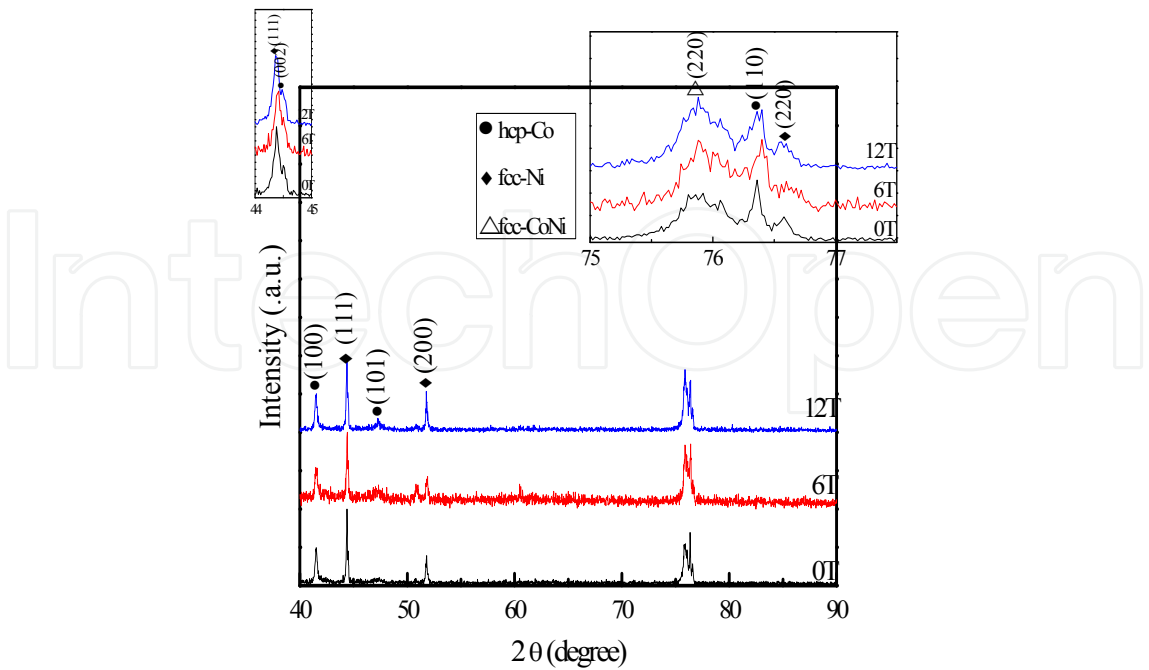


Figure 4. XRD patterns of 0.5 T-B_{ed} series Co/Ni films annealed under magnetic field of B_{annealing} = 0, 6, and 12 T. [48]

There is a general trend in the increase of fcc-CoNi peak (220) and the decreasing of hcp-Co peak (110) with increasing magnetic flux density during annealing process, as can be seen in the amplified zone of Figure 4 at the angular position from 2θ=75° to 77°. A higher volume fraction of CoNi alloy in a higher magnetic field was concluded not only from the increase of (200)CoNi compared to the (100)Co shown in Table 3 but also from the increase of diffusion zone according to the XPS composition analysis.

B _{annealing} (T)		0	6	12	
FCC-Ni	(111)	2θ (°)	44.44 ± 0.005	44.36 ± 0.011	44.42 ± 0.014
		FWHM	0.180 ± 0.002	0.183 ± 0.005	0.182 ± 0.004
	(200)	2θ (°)	51.84 ± 0.020	51.78 ± 0.012	51.84 ± 0.011
		FWHM	0.157 ± 0.003	0.165 ± 0.006	0.160 ± 0.002
	(220)	2θ (°)	76.64 ± 0.081	76.56 ± 0.014	76.62 ± 0.024
		FWHM	0.148 ± 0.008	0.161 ± 0.004	0.160 ± 0.007
HCP-Co	(100)	2θ (°)	41.54 ± 0.004	41.46 ± 0.013	41.54 ± 0.007
		FWHM	0.184 ± 0.002	0.234 ± 0.00	0.225 ± 0.009
	(110)	2θ (°)	76.40 ± 0.021	76.34 ± 0.02	76.40 ± 0.007
		FWHM	0.184 ± 0.008	0.365 ± 0.042	0.360 ± 0.029
FCC-CoNi	(220)	2θ (°)	76.60 ± 0.018	76.52 ± 0.032	76.49 ± 0.006
		FWHM	0.264 ± 0.010	0.365 ± 0.042	0.360 ± 0.029

Table 2. The width and position of the peaks under different magnetic annealing conditions.[48]

There is a general trend in the increase of fcc-CoNi peak (220) and the decreasing of hcp-Co peak (110) with increasing magnetic flux density during annealing process, as can be seen in the amplified zone of Figure 4 at the angular position from 2θ = 75° to 77°. A higher volume fraction of CoNi alloy in a higher magnetic field was concluded not only from the increase of (200)CoNi compared to the (100)Co shown in Table 3 but also from the increase of diffusion zone according to the XPS composition analysis.

$B_{\text{annealing}}$ (T)	fcc-CoNi (220)	hcp-Co (110)	fcc-Ni (220)
0	35.86%	45.52%	18.62%
6	40.53%	41.05%	18.42%
12	42.07%	39.80%	18.13%

Table 3. The dependence of intensity (I) ratio of the three peaks on the magnetic flux density during annealing process. In the table, Value = $I_{\text{fcc-CoNi}} / (I_{\text{fcc-CoNi}} + I_{\text{hcp-Co}} + I_{\text{fcc-Ni}}) \times 100\%$. [48]

The magnetism of the films in a magnetic field is favored for the transformation of $\epsilon(\text{hcp})$ structure to a more energetically stable $\alpha(\text{fcc})$ structure. The application of high magnetic field annealing induces a $\epsilon(\text{hcp}) \rightarrow \alpha(\text{fcc})$ phase transformation, which may account in the increase of thermal stability of the bilayered films [22].

1.4. Conclusion

Uniform nanocrystalline Co/Ni bilayered films were produced by the electrodeposition assisted with a 0.5 T weak magnetic field. Magnetic fields annealing of up to 12 T were selected in this study in order to investigate the high magnetic field effects on the evolution of morphology and microstructure of the films. A 0.5 T weak magnetic field parallel to the electrode induces modification of the deposits leading to changes in the grain size during magnetic field annealing. Grain shape in the Co/Ni morphology was modified with the grain boundary becoming clearer if a high magnetic field was applied during the annealing process. Atomic force microscopy investigations show that smaller grains and lower roughness are formed during annealing in the presence of a magnetic field comparing to the case of annealing without magnetic field. With increasing magnetic flux density during annealing process, the transformation from $\epsilon(\text{hcp})$ to $\alpha(\text{fcc})$ can be seen by the reduction of the ϵ -peak intensity, and the increase in that of α -peak. Overlapping effects of the high magnetic field annealing on diffusion, grain growth, alloying, and phase transformation have been discussed to interpret the experimental results.

Note: The main part, figures, and tables in **Section 1** have been published in Ref. [48].

2. The magnetic properties dependence on the coupled effects of magnetic fields on the microstructure of as-deposited and post-annealed Co/Ni bilayer films

2.1. Introduction

Nano-scaled metallic multilayers received great attention in the recent years because of their unique properties, such as mechanical, optical, electrical, and magnetic, with respect to commonly used alloys. Multilayer materials can be successfully produced by electrodeposition

[23], with thickness varying over a wide range from nanometric films [24-26] to micrometric coatings [27-30]. Moreover, with an accurate control of composition and thickness of each layer within the whole deposit, the internal stress that occurs usually in the microfilms can be reduced to a minimum level.

Electrodeposition is an effective method to produce cobalt-based alloys, but thin films obtained by this way contain some defects, such as rough surface. An application of parallel-to-electrode-surface magnetic field during the process can positively affect the deposits by smoothing their surfaces as well as improving magnetic properties [31-33]. This is caused by magnetohydrodynamic (MHD) and magnetocrystalline anisotropy effects. Magnetohydrodynamic convection induced by Lorentz force is considered as one of the characteristic phenomena in magneto-electrochemical processes [34, 35]. It is assumed that the forced convection resulting from the MHD effect decreases the thickness of the diffusion layer and enhances the concentration gradient, which improves the transport of ions toward the electrode surface. Uhlemann et al. [36] investigated the electrochemical deposition of Co-Cu/Cu multilayer under imposed magnetic field. They have reported that the deposition rate of Cu was nearly two times higher in the process carried out under magnetic field compared to the one without a B-field. Furthermore, the authors observed also an alignment of grains in (111) direction caused by the preferred orientation of Co during the electrodeposition in an external magnetic field. In other works [37-41], the magnetic field effects on nucleation, growth, texture, phase composition, and morphology of the Co layers have been noticed. It has been shown that a magnetic field applied during the deposition process is responsible for two different effects: first, field gradients attract ferromagnetic and paramagnetic materials and repel diamagnetic ones; second, even in uniform fields, magnetic dipoles and therefore the deposits align to the magnetic field direction [42,43]. Some researchers have pointed out that when changing the magnetic field to the orientation of perpendicular-to-electrode-surface, it leads to observe some micro-MHD effects [44]. It would affect roughness and morphology of thin films, while magnetizing force could influence already mentioned magnetic properties of deposits.

It is well known that the annealing process is of a great interest due to the possibilities to decrease an internal stress and to increase the chemical order in the film. In the case of bilayered films, new phases can appear. When the annealing process is carried out under magnetic field, the material properties can be strongly modified. As an example, the Ni-Co system studied by Wang et al. [45] can be given. It was found that the annealing process caused an increase in the wear loss, which was attributed to the decrease of hardness parameter as a result of an increase in the grain size during the high-temperature treatment. Kurant et al. [46] reported a dramatic decrease of magnetic anisotropy upon annealing that was caused by an enhanced diffusion at the metals' interfaces. Harada et al. [47] observed a magnetic field effect during the annealing process on the growth of grains in nanocrystalline Ni deposit produced by the electrodeposition method. Li et al. [48] and Yu et al. [49] determined the effect of vacuum magnetic annealing of Ni and Al co-doped ZnO films on structural and physical properties. Mikelson et al. [50] obtained the aligned solidification structure in Al-Cu and Cd-Zn alloys in a 1.5 T magnetic field. Savitisky et al. [51] and Li et al. [48] found the structure alignment along the direction of magnetic field. All these experimental research works have demonstrated that a magnetic field presents significant influence on the obtained materials.

The present work investigates the Co/Ni bilayered nanocrystalline films produced through the temperature-elevated electrochemical deposition, and modified by annealing carried out also under an external magnetic field. The results indicate an increase of the coercive field of deposited Co/Ni bilayers, when the electrodeposition process was conducted under a magnetic field of 1 T. The annealing processing caused further remarkable increase of the coercive field of as-prepared bilayers that has been preserved under magnetic annealing conditions. The magnetic properties are discussed in terms of samples microstructure. In as-prepared samples the in-plane magnetization was observed, while high temperature treatment, causing microstructural changes in the film, resulted also in appearance of a small component of magnetization oriented perpendicularly to the films' plane that could have been observed by MFM analysis. The induced perpendicular magnetization component in the post-annealed samples was a result of the magnetic field applied in the perpendicular direction to the samples' surface during annealing treatment.

2.2. Experimental methodology

The electrochemical experiments were performed in a conventional three-electrode cell. The working electrode (WE) was a square glass substrate of dimensions of 10 × 10 mm and 1.1 mm height, covered with ITO (In₂O₃:SnO₂) coating (electric contact layer) and embedded into a cylindrical holder. The counter electrode was made of a platinum plate and the reference electrode was a saturated mercury sulfate electrode (SSE). Electrodeposition process has been carried out in a cylindrical double-wall cell under the conditions listed in Table 4. The electrochemical cell was plunged into the gap of Drusch EAM 20G electromagnet, which delivers a uniform horizontal magnetic field parallel or perpendicular to the electrode surface.

System	Chemical agent	Concentration mol/L	Solution pH	Solution temperature °C	Current density mA/cm ²	Deposition time min	Magnetic field amplitude T	
							As-deposited	Post-annealed
Ni/ITO	NiSO ₄ ·7H ₂ O	0.6	2.7	30	-10	1	0	-
	H ₃ BO ₃	0.4						
Co/Ni/ITO	CoSO ₄ ·7H ₂ O	0.6	4.7	50	-10	1	1	≤12
	H ₃ BO ₃	0.4						

Table 4. Processing conditions for the Co/Ni bilayer thin films. [56]

The electrodeposition process included two steps, which were related to: firstly - deposition of Ni seed-layer directly on ITO/glass substrate, secondly - deposition of Co layer. The Ni seed-layer deposition was undertaken without an applied magnetic field, while the Co layers deposition was performed under superimposition of a magnetic field with the strength up to 1 T in parallel-to-electrode-surface orientation. Thicknesses of the layers were determined

according to the X-Ray photoelectron spectroscopy (XPS) measurements done for the similar, but thicker than considered here, Co/Ni layers reported in Ref. [52]. The difference between these two investigated systems is the deposition time, which in [52] was longer: 6 min deposition of Ni seed layer and 4 min deposition of Co proper layer, respectively. Thus, based on this the estimated thickness of layers considered in this work is approximately 200 nm for Ni and 300–400 nm for Co layer, depending on the magnetic field intensity. Additionally, the roughness of Ni seed-layer determined by AFM was $40 \pm 3 \text{ nm}$, while the roughness of Co secondary layer was $38 \pm 2 \text{ nm}$ when the process was carried out without a superimposed magnetic field. Then, roughness of the Co layer has been slightly improved (decreased) when electrodeposition was carried out under superimposed magnetic field: $\sim 35 \text{ nm}$ (± 3) and 29 nm (± 2) under 0.5 and 1 T, respectively. The electrolyte pH was adjusted to proper level by addition of sulfuric acid or sodium hydroxide. Besides the basic salts no other chemical additives, which are usually used to avoid the effect of hydrogen evolution on the films morphology, were added. Boric acid, in addition to its buffer function, is a useful additive compound favoring the formation of low roughness deposits. All of the electrochemical investigations were carried out using the chronopotentiometry method, where a constant current density of -10 mA/cm^2 was applied. The potential of working electrode was controlled by means of a potentiostat-galvanostat VersaSTAT4. The heat treatment process of Co/Ni bilayered films was carried out in a vertical furnace placed into the superconducting magnet with strength up to 12 T and perpendicular magnetic field flux to the samples surface. The films were annealed at 673 K during 4 h under a protective atmosphere of high-purity argon and then cooled down to the room temperature. Bruker D8 Advance and GI-XRD Ultima IV X-ray Diffractometers with $\text{CuK}\alpha$ radiation have been employed to obtain XRD patterns using standard θ - 2θ geometry. Microstructures of the obtained layers have been investigated by field emission scanning electron microscopy (FE-SEM) Supra 35, Japan. The hysteresis loops have been measured by means of a vector VSM (LakeShore 7410) and an alternating gradient field magnetometer (AGFM, PMC 2900) and the magnetic field has been applied in the in-plane configuration. Magnetic force microscopy (MFM, Bruker Multimode V Nanoscope 8) analysis has been performed in tapping-lift mode with CoCr-coated tips.

2.3. Results and discussion

In order to determine the effects of magnetic fields superimposed during both electrodeposition and annealing processes on the magnetic properties of Co/Ni/ITO bilayer films, room temperature in-plane hysteresis loops were recorded. Figure 5 indicates the magnetic characteristic of as-prepared Co/Ni/ITO films.

It is observed that film deposited under 1 T magnetic field tends to be slightly more difficult to magnetize than film deposited in the absence of an external magnetic field. An increase in coercivity (H_c), from 45 Oe (As-deposited, 0 T) to 78 Oe (As-deposited, 1 T) is noticed, when a magnetic field was superimposed during electrodeposition. The occurred variation in the coercive field cannot be attributed to induced magneto-crystalline anisotropy, as is usually the case in physical deposition processes under the application of a magnetic field. In fact, no significant dependence of the magnetic properties is observed along different directions of the

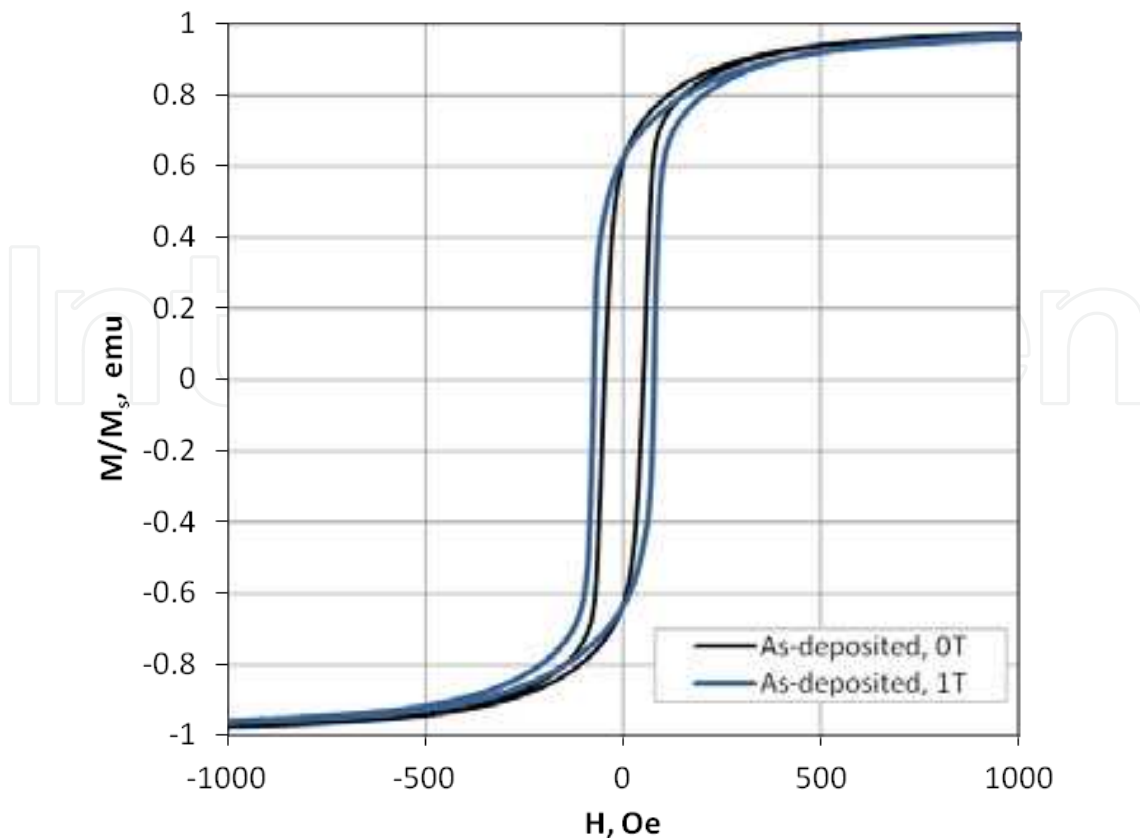


Figure 5. Comparison of the hysteresis loops of Co/Ni/ITO bilayer films electrodeposited without and with a superimposed magnetic field.[56]

applied magnetic field, in the sample plane. Instead, electrochemical deposition under magnetic field affects locally the chemical environment surrounding the magnetic atoms and the mechanisms of grain growth; therefore, the increased value of H_c might be explained in terms of a possible variation of the shape anisotropy of the Co crystals, as reported in [53], or to a slightly larger crystal size when deposition occurs under an applied magnetic field. One of the key issues for the dependence of coercivity on the grain size is the domains around grain boundaries. The rearrangement of the domains costs some energy and therefore contributes to coercivity [54]. The relative volume of the grain boundary domains increases with the increasing of the magnetocrystalline anisotropy, consequently leading to a rise in coercivity.

Both samples were then annealed under magnetic conditions and the hysteresis loops were again recorded. In both cases, as-deposited Co/Ni/ITO films under 0 and 1 T magnetic field, a significant increase of the coercive fields was observed. At the same time, a slower approach to the saturation has been noticed, which is probably due to the increased intermixing of Co and Ni atoms at the interfaces, since their existence has been proven and discussed in Ref. [54]. An increased H_c is mostly associated with the mixed effects of recrystallization process and structural modifications. Further annealing under magnetic conditions of 6 and 12 T brings about only a slight increase of the H_c value (Figure 6), which is most likely to be caused by enhanced increase of Co grains and structural directionality. However, the presence of an interdiffusion zone between Co and Ni layers cannot be neglected as well. In any case, no

significant induced magnetocrystalline anisotropy seems to come from the field annealing procedure, as the final coercivity values are mostly independent of the application of a magnetic field during annealing.

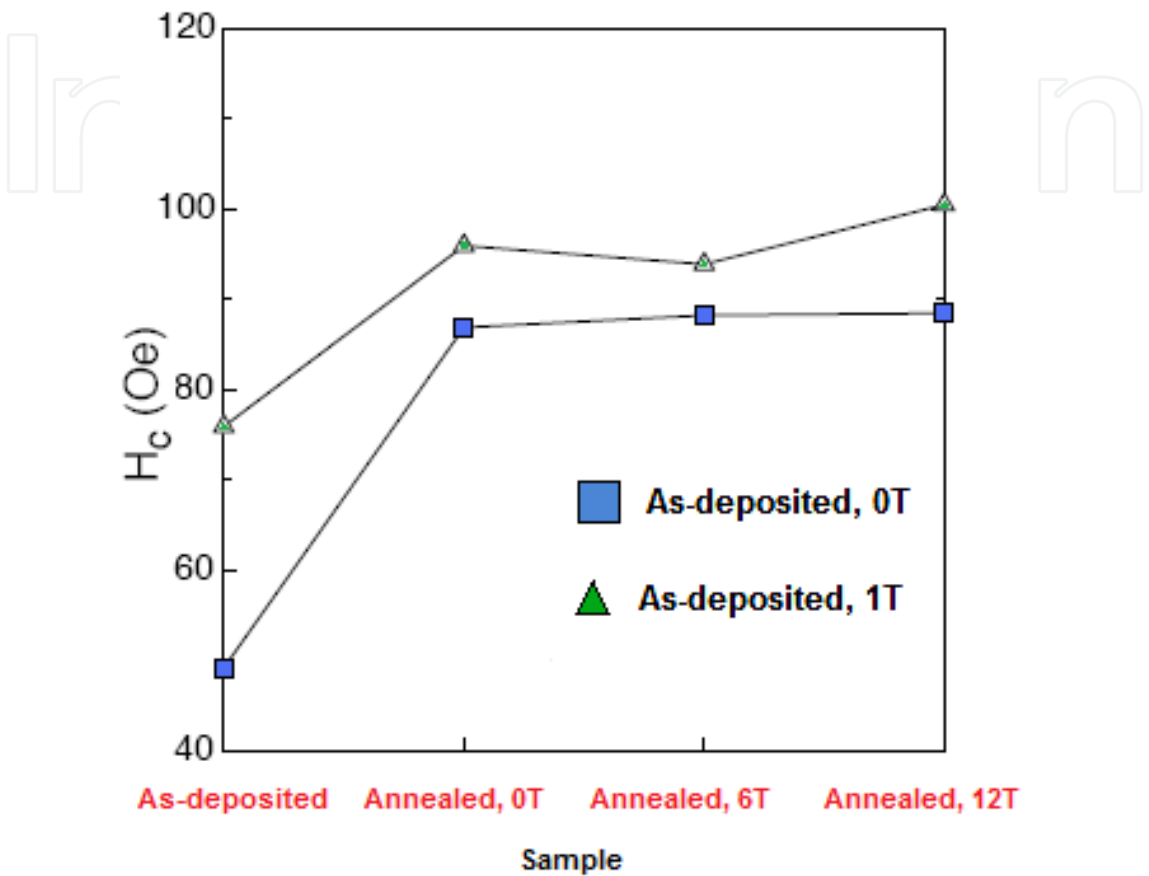


Figure 6. Comparison of the coercivity field of Co/Ni/ITO bilayer films before (as-deposited) and after (post-annealed) annealing treatment.[56]

Extended analysis of the magnetic characteristics of post-annealed Co/Ni/ITO bilayer films have been done by use of magnetic force microscopy (MFM). All samples have been investigated at their in-plane remanence, after a saturating magnetic field has been applied. The MFM tip is magnetized perpendicular to the sample plane; therefore, the MFM is sensitive to the second derivative of the z component of the field generated by the sample magnetization in the half space above the sample surface. The images report in false colors the phase channel in pass 2 (retrace) at a lift scan height of 50 nm. Figure 7 presents MFM images of the Co/Ni/ITO films as-deposited and post-annealed, respectively, on the base of AFM images presented in Figure 2. The magnetic structure consists of bubble-like domains - small, cylindrical magnetic domains that are usually formed when an external magnetic field is applied perpendicularly to the surface of the film. In general, the domains run in random directions in the film plane, i.e., no directionality in the orientation of domains is observed. The domains are displayed as bright and dark areas and have opposite magnetization components perpen-

pendicular to the film surface. For the sample deposited under no magnetic field, annealing is responsible for a severe change of the domain structure that is not significantly affected by the application of a magnetic field, in agreement with the coercivity values reported in Figure 6. In particular, the magnetic features size considerably reduces with respect to the as-deposited film, whereas the increased magnetic contrast (as documented by the very different color scales in the top row images in Figure 7) can be attributed to a stronger anisotropy within the individual grains, in turn responsible for the increase of H_c . The Co/Ni films' exposure on the high-temperature treatment changes their microstructure in means of grains' growth. Under thermal conditions, the grains of as-deposited films that were mostly agglomerated into islands begin to grow separately due to the broken symmetry at the interfaces. As a result, ultra-thin magnetic layers tend to be perpendicularly magnetized. Additional contribution might also come from dipolar interaction between the grain islands in the film. In consequence, the observed increasing anisotropy is a result of the single grains growth that boundaries become more clear and visible, and thus, the increased magnetic contrast is observed.

No preferred orientation of the anisotropy is observed even under the application of a 12 T field during annealing. For the sample deposited under the application of a 1 T field on the sample plane, the magnetic features in the as-prepared state are very different with respect to the sample deposited in 0 field, because of the different grain growth mechanisms.

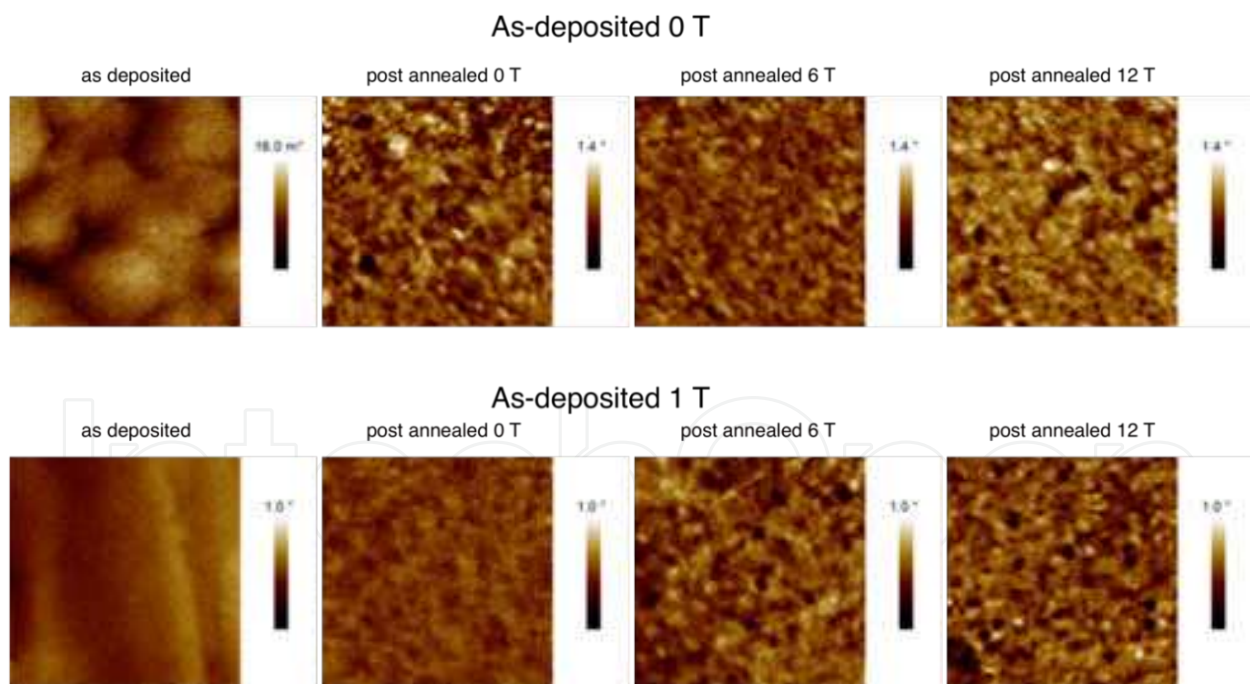


Figure 7. MFM analysis of the Co/Ni/ITO films. The lateral size of each image is 5 μm . [56]

However, after annealing a domain configuration similar to the other sample is obtained, again with no significant dependence on the field intensity applied during annealing. The slightly reduced color scale in the images of the bottom row of Figure 7 with respect to those of the top row account for a slightly lower anisotropy value of the Co grains, which is in agreement with

the slightly lower coercivity reported in Figure 6. Moreover, a 2D power spectral density [55] calculated on the MFM images of Figure 7 reports a slight decrease of the magnetic features size after annealing, as evidenced in Figure 8 for two examples, as-prepared sample and annealed at 6 T.

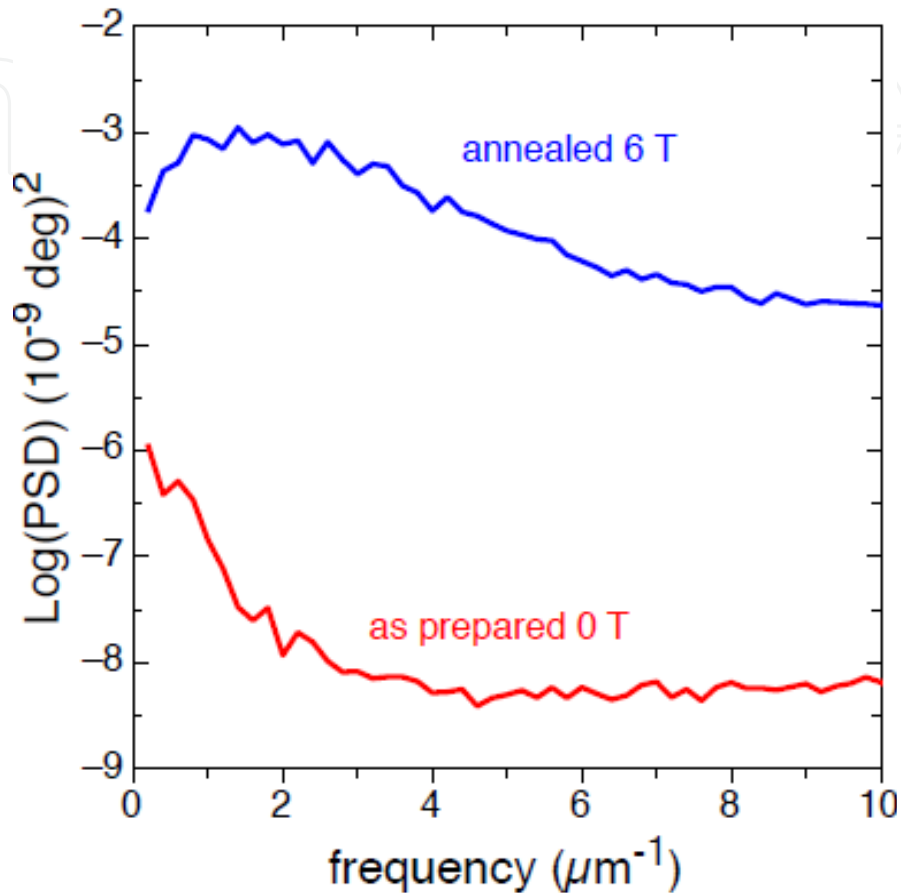


Figure 8. 2D power spectral density of the as-prepared and post-annealed Co/Ni/ITO films.[56]

The appearance of a maximum in the blue curve at higher frequencies (shorter wavelengths) marks the decrease of magnetic features size that can be attributed to a slight increase of the magnetic anisotropy with annealing; a similar behavior has been observed in L₁₀ Fe-Pt films [55]. This is in agreement with the measured hysteresis loops, as discussed in Figures 5 and 6. The observed magnetic anisotropy is probably due to the magnetic interactions among the grains: in fact, MFM images (Figure 7) reveal that the magnetic features are larger than the individual grains (AFM images, Figure 2); an increase of the grain size as a consequence of the annealing process increases the dipolar coupling energy among the grains: they are no longer agglomerated into island, but grow separately with larger volume of grain boundaries that results in easier magnetic interaction between them.

In consequence, increasing effective magnetic anisotropy is observed, in agreement with Figure 7, where most grains have preferred orientations in the presence of an external magnetic field. Thus, the magnetic domain structure determines the hysteresis loops of Co/Ni/ITO films,

and the domains configuration is affected by the surface morphology, while their reduced size is probably affected by structural defects, such as grain boundaries and impurities.

2.4. Conclusion

The coupled effects of a superimposed magnetic field during both electrodeposition and magnetic annealing treatment in dependence on Co/Ni/ITO microstructure were investigated. The magnetic fields applied in the two processes (growth and annealing) play very different roles. During growth, the modified electrochemical environment around the electrode is responsible for the deposition of Co atoms in islands having a different size and shape anisotropies that result in a higher coercivity. Conversely, it has been shown that the crystallographical structure of as-deposited films is improved by annealing treatment that induces the recrystallization effect. A superimposed magnetic field during annealing promotes diffusion of atoms between Co and Ni layers. The magnetic field annealing has affected the magnetic properties of Co/Ni/ITO films by minimizing the magnetic anisotropy energy of the systems due to the stress relief between grains and directional atomic pair ordering. The direction bonds of dissimilar atoms (Co, Ni) in the films may affect their asymmetric distribution under superimposed magnetic field, when supposing that its strength is sufficiently high. Furthermore, the magnetic field annealing increases the dipolar interactions between metals grains and the redistribution of pair ordering directions, which are perpendicular to the magnetization direction in each domain, as in the case of Co/Ni/ITO films, can be observed. An increased magnetic anisotropy in the investigated films was always obtained after annealing, with coercive fields up to about 100 Oe.

Note: The main part, figures, and tables in **Section 2** have been published in Ref. [56].

3. Influence of high magnetic field annealing on the microstructure of pulse-electrodeposited nanocrystalline Co-Ni-P films

3.1. Introduction

The electrodeposited Co-Ni-P film is a promising magnetic material for micro-electro-mechanical systems (MEMS) [57] and magnetic recording media [58]. The alloy film preparation by pulse electrodeposition method [59] presents the advantage of a nanocrystalline regime and a fine magnetic property, with a low production cost. However, the nonequilibrium state of the as-electrodeposited nanocrystalline layers, in another word, the strong thermodynamic potential for grain growth, may be a limiting factor in the successful applications of this functional film. Recently, the possibility of controlling the grain growth and improving the thermal stability in the as-deposited films by using magnetic field annealing was reported [60 - 62]. Harada et al. [63] annealed the electrodeposited nanocrystalline Ni under a 1.2 MA/m field and found grain growth could not occur after the early stage. Few applications of high magnetic field during annealing process [64] prove it a promising method to tailor the final

microstructure (e.g., surface topography, grain size, crystallographic orientation). In this work, we focus on the microstructure evolution of pulsed-electrodeposited Co-Ni-P film during the magnetic annealing process.

3.2. Experimental

The bath (pH = 3.7) for the electrodeposition of CoNiP films consisted of 0.91 M $\text{NiSO}_4 \cdot 6\text{H}_2\text{O}$, 0.17 M $\text{NiCl}_2 \cdot 6\text{H}_2\text{O}$, 0.11 M $\text{CoSO}_4 \cdot 7\text{H}_2\text{O}$, 0.48 M H_3BO_3 , 0.29 M NaH_2PO_2 , and 0.0035 M $\text{C}_{12}\text{H}_{25}\text{NaO}_4\text{S}$. All electrochemical experiments were performed in a conventional two-electrode cell without agitation. The cathode was Cu plate ($10 \times 10 \times 1$ mm) with a seed layer Ni (~60 nm), which was prepared by the physical vacuumed deposition (PVD) method. A nickel plate with area of 2 cm^2 was used as the anode. A unidirectional rectangle pulse current was used, the current was 0.01 A and the duty ratio was 1:5. The pulse-electrodeposition was performed at room temperature for 30 min. After electrodeposited, the samples were heat-treated at 673 K for 4 h under a protective atmosphere of high-purity argon in a vertical furnace, which was placed inside a superconducting magnet. The direction of the external magnetic field was in perpendicular to the surface of the films, and the applied magnetic flux density (B) during the annealing process was up to 9 T. Surface morphology of the Co-Ni-P alloy thin films were observed by field emission scanning electronic microscopy (FE-SEM, SUPRA 35, German). To quantitatively analyze the grain size and the roughness of the films, atomic force microscopy (AFM, NTEGRA AURA, NT-MDT, Russia) was used in the area of $15 \times 15 \mu\text{m}$ at three different positions to obtain average data. The crystal structure was detected by grazing incidence X-ray diffraction (GI-XRD, Ultima IV, Japan) using $\text{Cu } K\alpha_1$ radiation (40 kV, 40 mA, $0.02^\circ/\text{step}$).

3.3. Results and Discussion

3.3.1. Surface morphology

In Figure 9, surface morphologies of the as-deposited Co-Ni-P film and the annealed films with and without high magnetic field were observed by FE-SEM. It was apparent that the annealing process, whether with or without a magnetic field, induced an obvious evolution in the morphology of the as-electrodeposited film. The as-deposited Co-Ni-P film (Figure 9 (a)) shows a kind of grape-like structure that combined of spherical clusters with different sizes, meanwhile, the surface of the as-deposited film was rough and inhomogeneous. After annealed at 673 K, the small grains in the clusters coalesced together to form bigger grains, with the small grains vanishing at the edges of the bigger grains due to a recrystallization process. However, a 9 T magnetic field annealing favored to form a more uniform surface with smaller grain size and lower roughness, compared with the annealed samples obtained in the absence of magnetic field. The white dots in Figure 9 (b) were phosphorus grains separated out from the alloy, which dots disappeared when a 9 T magnetic field was applied during annealing process. The influencing mechanisms of high magnetic field annealing on the morphology evolution in the CoNiP electrodeposits can be interpreted in terms of the overlapping effects: diffusion and recrystallization. On one side, the introduction of the

magnetization energy during the magnetic field annealing decreased the diffusion activation energy [65], resulting in an acceleration effect on diffusion. On the other side, owing to the fact that the retarded effect of a 9 T strong magnetic field on the recrystallization process plays a more important role against its acceleration effect on diffusion process [66–67], the coalescence and growth of small grains were suppressed.

in the area of $15\times15\text{ }\mu\text{m}^2$ at three different positions to obtain average data. The crystal structure was detected by grazing incidence X-ray diffraction (GI-XRD, Ultima IV, Japan) using Cu $K\alpha_1$ radiation (40 kV, 40 mA, 0.02°/step).

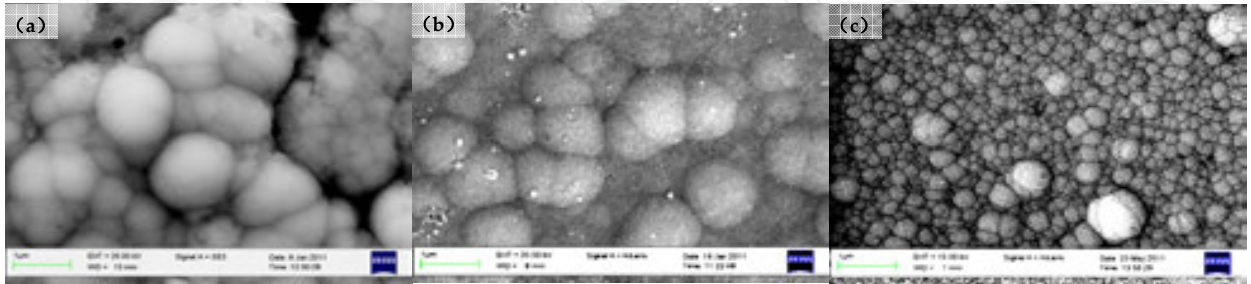


Figure 9. Typical FE-SEM images of as deposited CoNiP thin film (a) and post-annealed in the case of: (b) B = 0 T, (c) B = 9 T.

In Figure 9., surface morphologies of the as-deposited Co-Ni-P film and the annealed films with and without high magnetic field were observed by FE-SEM. It was apparent that the annealing process, whether with or without a magnetic field, induced an obvious evolution in the morphology of the as-electrodeposited film. The as-deposited Co-Ni-P film (Figure 9 (a)) shows a kind of grape-like structure that combined of spherical clusters with different sizes, meanwhile, the surface of the as-deposited film was rough and inhomogeneous. After annealed at 673 K, the small grains in the clusters coalesced together to form bigger grains, with the small grains vanishing at the edges of the bigger grains due to a recrystallization process. However, a 9 T magnetic field annealing favored to form a more uniform surface with smaller grain size and lower roughness, compared with the annealed samples obtained in the absence of magnetic field. The white dots in Figure 9 (b) were phosphorus grains separated out from the film, which were disappeared when a magnetic field was applied during annealing process. The average grain size and the average roughness were calculated by standard Nova software attached on the AFM setup. According to the values in Table 5, it was obvious that no significant increase in the grain size of the film after annealed during the magnetic field annealing decreased the diffusion activation energy [65], resulting in an acceleration effect on diffusion. On the other side, owing to the fact that the retarded effect of a 9 T strong magnetic field on the recrystallization process plays a more important role against its acceleration effect on diffusion process [66–67], the coalescence and growth of small grains were suppressed.

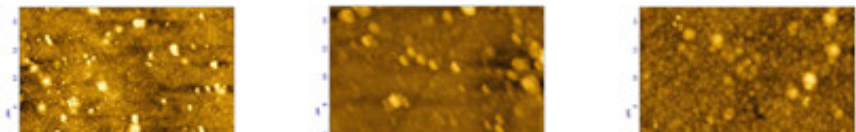
3.3.2. Average grain size and roughness

In order to quantitatively analyze the roughness and the grain size of the CoNiP films, AFM top view and three-dimensional image of the nanocrystalline films, before annealed, and annealed at different magnetic flux densities (0 T, 9 T) are shown in Figure 10. On the surface of all the films, most grains were in spherical shape with crack-free. Comparing with the as-deposited film, the grain size and roughness in the case of no-field annealing increased dramatically. While the application of 9 T magnetic field during annealing process leads to a decrease in grain size and surface roughness. The average grain size and the average roughness were calculated by standard Nova software attached on the AFM setup. According to the values in Table 5, it was obvious that no significant increase in the grain size of the film after annealed during the magnetic field annealing decreased the diffusion activation energy [65], resulting in an acceleration effect on diffusion. On the other side, owing to the fact that the retarded effect of a 9 T strong magnetic field on the recrystallization process plays a more important role against its acceleration effect on diffusion process [66–67], the coalescence and growth of small grains were suppressed.

As deposited			Annealed at 9 T (0 T)		
crack-free. Comparing with the as-deposited film, the grain size and roughness in the case of no-field annealing increased dramatically. While the application of 9 T magnetic field during annealing process leads to a decrease in grain size and surface roughness. The average grain size and the average roughness were calculated by standard					
Grain size (nm)	32.2±3.4		97.53±5.5		44.6±2.6
Roughness (nm)	9.15±0.72		16.35±1.02		8.88±0.56

Table 5. Grain size and roughness of the CoNiP films, before annealed and post-annealed under a 0 T or 9 T magnetic field.

In order to quantitatively analyze the roughness and the grain size of the CoNiP films, AFM top view and three-dimensional image of the nanocrystalline films, before annealed, and annealed at different magnetic flux densities (0 T, 9 T) are shown in Figure 10. On the surface of all the films, most grains were in spherical shape with crack-free. Comparing with the as-deposited film, the grain size and roughness in the case of no-field annealing increased dramatically. While the application of 9 T magnetic field during annealing process leads to a decrease in grain size and surface roughness. The average grain size and the average roughness were calculated by standard Nova software attached on the AFM setup. According to the values in Table 5, it was obvious that no significant increase in the grain size of the film after annealed during the magnetic field annealing decreased the diffusion activation energy [65], resulting in an acceleration effect on diffusion. On the other side, owing to the fact that the retarded effect of a 9 T strong magnetic field on the recrystallization process plays a more important role against its acceleration effect on diffusion process [66–67], the coalescence and growth of small grains were suppressed.



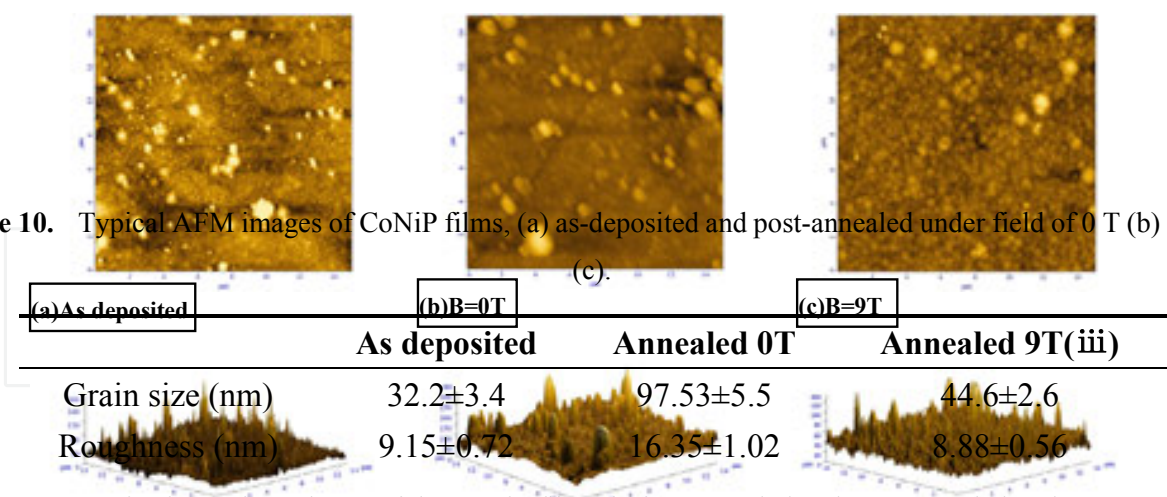


Figure 10. Typical AFM images of CoNiP films, (a) as-deposited and post-annealed under field of 0 T (b) and 9 T (c).

Table 5. Grain size and roughness of the CoNiP films, before annealed and post-annealed under a 0 T or 9 T

Figure 10. Typical AFM images of CoNiP films, (a) as-deposited and post-annealed under field of 0 T (b) and 9 T (c).

Figure 10. Typical AFM images of CoNiP films, (a) as-deposited and post-annealed under field of 0 T (b) and 9 T (c).

3.3.3.3 Crystal structure

The XRD patterns of as deposited and post-annealed samples were shown in Figure 11. The magnified diffraction pattern between 42° and 48° of 2θ is shown in the inset of (A). The XRD patterns of as deposited, annealed 0 T, and annealed 9 T (iii) were shown in Figure 11. The magnified diffraction pattern between 42° and 48° of 2θ is shown in the inset of (A).

Table 5. Grain size and roughness of the CoNiP films, before annealed and post-annealed under a 0 T or 9 T magnetic field.

3.3.3 Crystal structure

The XRD patterns of as deposited and post-annealed samples were shown in Figure 11. The magnified diffraction pattern between 42° and 48° of 2θ is shown in the inset of (A).

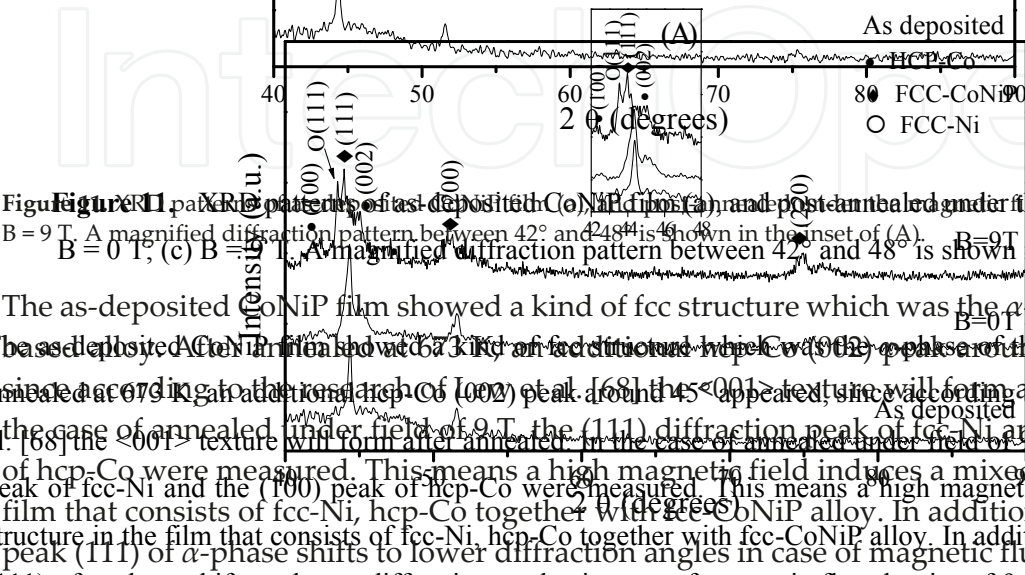


Figure 11. XRD patterns of as-deposited CoNiP film (a) and post-annealed under magnetic field of (b) B = 9 T, (c) B = 0 T, and (d) B = 9 T. A magnified diffraction pattern between 42° and 48° is shown in the inset of (A).

The as-deposited CoNiP film showed a kind of fcc structure which was the α phase of the Co-based alloy. After annealing, a kind of additional hcp-Co (002) peak of the Co-based alloy appeared. According to the research of [68], the $\langle 001 \rangle$ texture will form after annealing. In the case of annealed under field of 9 T, the (111) diffraction peak of fcc-Ni and the (100) peak of hcp-Co were measured. This means a high magnetic field induces a mixed structure in the film that consists of fcc-Ni, hcp-Co together with fcc-CoNiP alloy. In addition, the diffraction peak (111) of α -phase shifts to lower diffraction angles in case of magnetic flux density of 9 T. (111) of fcc-Ni shifts to lower diffraction angles in case of magnetic flux density under 9 T. This behavior can be rationalized as more Ni atoms are separated from CoNiP solid solution under a high magnetic field, resulting in a transition from Ni-like fcc-microstructural evolution to Co-like fcc-microstructural [69]. The XRD results reveal that the as-deposited CoNiP film showed a kind of fcc structure, which was the α phase of the Co-based alloy. After annealing, a kind of additional hcp-Co (002) peak of the alloy and an increasing effect of high magnetic field on diffusion modified this trend. By the way, during the annealing under a field of 9 T, the (111) diffraction

This behavior can be rationalized as more Ni atoms are separated out of the CoNiP solid solution under a high magnetic field, resulting in a transition from Ni-like fcc-microstructural evolution to Co-like fcc-microstructural [69]. The XRD results reveal that during the electro-deposition process, the structure of supersaturated solid solution CoNiP (α -phase), is not stable. After annealing, Ni and Co atoms have a potential to separate out of the alloy, and an accelerating effect of high magnetic field on diffusion modifies this tendency during the annealing process.

3.4. Conclusion

We have studied the influence of high magnetic field annealing on the grain growth and phase structure of pulse electrodeposition CoNiP films. FE-SEM and AFM studies showed that the grains size and the roughness were decreased after annealed under the high magnetic field. X-ray diffraction patterns showed that a mixed phase structure was formed in the annealed film under a 9 T magnetic field.

Note 1: The main part, figures, and tables in **Section 3** have been published on Journal of Iron and Steel Research as: Li DG, Chun WU, Qiang W, Agnieszka F, He J-C. Influence of high magnetic field annealing on microstructure of pulse-electrodeposited nanocrystalline Co-Ni-P films. J Iron Steel Res Int 2012;19:1085-8.

Note 2: The three sections in Chapter one is mainly about the influence of post-annealing under high magnetic fields on the microstructure of pulse-electrodeposited nanocrystalline Co-based films.

Author details

Donggang Li^{1,3*}, Qiang Wang^{2*}, Agnieszka Franczak³, Alexandra Levesque³ and Jean-Paul Chopart³

*Address all correspondence to: lidonggang@smm.neu.edu.cn, wangq@mail.neu.edu.cn

1 School of Materials and Metallurgy, Northeastern University, Shenyang, China

2 Key Laboratory of Electromagnetic Processing of Materials (Ministry of Education), Northeastern University, Shenyang, China

3 LISM, Université de Reims Champagne-Ardenne, France

References

- [1] Baghbanan M, Erb U, Palumbo G. In: Mukhopadhyay SM, Seal S, Dahotre N, Agarwal A, Smugeresky JE, Moody N. (eds.) Surface and Interfaces in Nanostructured

- Materials and Trends in LIGA, Miniaturization and Nanoscale Materials, The Minerals, Metals and Materials Society, Warrendale, PA, 2004, pp. 307-315.
- [2] Cavallotti PL, Vincenzo A, Bestetti M, Franz S. Microelectrodeposition of cobalt and cobalt alloys for magnetic layers, *Surf Coat Technol* 2003;73:169-70.
 - [3] Tian L, Xu J, Qiang C. The electrodeposition behaviors and magnetic properties of Ni-Co films, *Appl Surf Sci* 2011;257:4689-94.
 - [4] Koza JA, Karnbach F, Uhlemann M, McCord J, Mickel C, Gebert A, Baunack S, Schultz L. Electrocrystallisation of CoFe alloys under the influence of external homogeneous magnetic fields—Properties of deposited thin films, *Electrochim Acta* 2010;55:819-31.
 - [5] Georgescu V, Daub M. Magnetic field effects on surface morphology and magnetic properties of Co-Ni-P films prepared by electrodeposition, *Surf Sci* 2006;60:4195-9.
 - [6] Krause A, Hamann C, Uhlemann M, Gebert A, Schultz L. Influence of a magnetic field on the morphology of electrodeposited cobalt, *Magn Magn Mater* 2005;290-291:261-4.
 - [7] Hibbard G, Erb U, Aus KT, Klement U, Palumbo G. Thermal stability of nanostructured electrodeposits, *Mater Sci Forum* 2002;386-388:387-96.
 - [8] Li YB, Lou YF, Zhang LR, Ma B, Bai JM, Wei FL. Effect of magnetic field annealing on microstructure and magnetic properties of FePt films, *J Magn Magn Mater* 2010 ; 322:3789-91.
 - [9] Markou A, Panagiotopoulos I, Bakas T. Effects of layering and magnetic annealing on the texture of CoPt films, *J Magn Magn Mater* 2010 ;322:L61-3.
 - [10] Li DS, Garmestani H, Yan S-S, Elkawni M, Bacaltchuk MB, Schneider-Muntau HJ, Liu JP, Saha S, Barnard JA. Effects of high magnetic field annealing on texture and magnetic properties of FePd, *J Magn Magn Mater* 2004;281:272-5.
 - [11] Liu T, Li D, Wang Q, Wang K, Xu Z, He J. Enhancement of the Kirkendall effect in Cu-Ni diffusion couples induced by high magnetic fields, *J Appl Phys* 2010;107:103542(1-3).
 - [12] Li D, Wang Q, Liu T, Li G, He J. Growth of diffusion layers at liquid Al-solid Cu interface under uniform and gradient high magnetic field conditions, *Mater Chem Phys* 2009;117:504-10.
 - [13] Li D, Wang Q, Li G, Lv X, Nakajima K, He J. Diffusion layer growth at Zn/Cu interface under uniform and gradient high magnetic fields, *Mater Sci Eng A* 2008;495:244-8.
 - [14] Coey JMD, Hinds G. Magnetic electrodeposition, *J Alloy Compd* 2001;326:238-45.

- [15] Tang X, Dai J, Zhu X, Song W, Sun Y. Magnetic annealing effects on multiferroic Bi-FeO₃/CoFe₂O₄ bilayered films, *J Alloy Compd* 2011;511:4748-53.
- [16] Martikainen HO, Lindroos VK. Observations of the effect of magnetic field on the recrystallization in ferrite, *Scand J Metall* 1981;10(1):3-8.
- [17] Xu Y, Ohtsuka Y, Wada H. Effects of a strong magnetic field on diffusional transformations in Fe-based alloys, *J Mag Soc Jpn* 2000;24(4):655-8.
- [18] Molodov DA, Bhaumik S, Molodova X, Gottstein G. Annealing behaviour of cold rolled aluminum alloy in a high magnetic field, *Scripta Mater* 2006;54(12):2161-4.
- [19] Hu C-C, Wu C-M. Effects of deposition modes on the microstructure of copper deposits from an acidic sulfate bath, *Surf Coat Technol* 2003;176:75-83.
- [20] Zhao J, Yang P, Zhu F, Cheng C. The effect of high magnetic field on the growth behavior of Sn-3Ag-0.5Cu/Cu IMC layer, *Scripta Mater* 2006;54(6):1077-80.
- [21] Cullity BD. Elements of X-ray Diffraction, 2nd edn, Addison Wesley Publishing Company, Inc, London, 1978.
- [22] Hibbard GD, Aust KT, Erb U. Thermal stability of electrodeposited nanocrystalline Ni-Co alloys, *Mater Sci Eng A* 2006;433:195-202.
- [23] Yamada A, Houga T, Ueda Y. Magnetism and magnetoresistance of Co/Cu multilayer films produced by pulse control electrodeposition method, *J Magn Magn Mater* 2002;239:272-5.
- [24] Herman AM, Mansour M, Badri V, Pinkhasov P, Gonzales C, Fickett F, Calixto ME, Sebastian PJ, Marshall CH, Gillespie TJ. Deposition of smooth Cu(In,Ga)Se₂ films from binary multilayers, *Thin Solid Films* 2000;361-362:74-8.
- [25] Toth Kadar E, Peter L, Becsei T, Schwarzacher W. Preparation and magnetoresistance characteristics of electrodeposited Ni-Cu alloys and Ni-Cu/Cu multilayers, *J Electrochem Soc* 2000;147:3311-18.
- [26] Gomez E, Labarta A, Llorente A, Valles E. Electrochemical behaviour and physical properties of Cu/Co multilayers, *Electrochim Acta* 2003;48:1005-13.
- [27] Kirilova I, Ivanov I, Rashkov S. Anodic behaviour of one and two-layer coatings of Zn and Co electrodeposited from single and dual baths, *J Appl Electrochem* 1998;28:637-43.
- [28] Jensen JD, Gabe DR, Wilcox GD. The practical realisation of zinc-iron CMA coatings, *Surf Coat Technol* 1998;105:240-50.
- [29] Kalantary MR, Wilcox GD, Gabe DR. Alternate layers of zinc and nickel electrodeposited to protect steel, *Br Corrosion J* 1998;33:197-201.

- [30] Wang L, Gao Y, Xue Q, Liu H, Xu T. Graded composition and structure in nanocrystalline Ni-Co alloys for decreasing internal stress and improving tribological properties, *J Phys D: App Phys* 2005;38:1318-24.
- [31] Armyanov S. Crystallographic structure and magnetic properties of electrodeposited cobalt and cobalt alloys, *Electrochim Acta* 2000;45:3323-35.
- [32] Cavallotti PL, Vincenzo A, Bestetti M, Franz S. Microelectrodeposition of cobalt and cobalt alloys for magnetic layers, *Surf Coat Technol* 2003;169:76-80.
- [33] Yu Y, Wei G, Hu X, Ge H, Yu Z. The effect of magnetic fields on the electroless deposition of Co-W-P film, *Surf Coat Tech* 2010;204:2669-76.
- [34] Chopart J-P, Olivier A, Merienne E, Amblard J, Aaboubi O. New experimental device for convective mass-transport analysis by electrokinetic-hydrodynamic effect, *Electrochem Sol Sta Lett* 1998;1:139-41.
- [35] Levesque A, Chouchane S, Douglade J, Rehamnia R, Chopart J-P. Effect of natural and magnetic convections on the structure of electrodeposited zinc-nickel alloy, *App Surf Sci* 2009;255:8048-53.
- [36] Uhlemann M, Gebert A, Herrich M, Krause A, Cziraki A, Schultz L. Electrochemical deposition and modification of Cu/Co-Cu multilayer, *Electrochim Acta* 2003;48:3005-11.
- [37] Krause A, Uhlemann M, Gebert A, Schultz L. A study of nucleation, growth, texture and phase formation of electrodeposited cobalt layers and the influence of magnetic fields, *Thin Solid Films* 2006;515:1694-700.
- [38] Krause A, Hamann C, Uhlemann M, Gebert A, Schultz L. Influence of a magnetic field on the morphology of electrodeposited cobalt, *J Magn Magn Mat* 2005;290:261-4.
- [39] Franczak A, Levesque A, Bohr F, Douglade J, Chopart J-P. Structural and morphological modifications of the Co-thin films caused by magnetic field and pH variation, *App Surf Sci* 2012;258:8683-8.
- [40] Li D, Levesque A, Franczak A, Wang Q, He J, Chopart J-P. Evolution of morphology in electrodeposited nanocrystalline Co-Ni films by in-situ high magnetic field application, *Talanta* 2013;110(15):66-70.
- [41] Koza JA, Uhlemann M, Gebert A, Schultz L. Nucleation and growth of the electrodeposited iron layers in the presence of an external magnetic field, *Electrochim Acta* 2008;53:7972-80.
- [42] Li X, Ren Z, Fautrelle Y. Alignment behavior of the primary Al₃Ni phase in Al-Ni alloy under a high magnetic field, *J Crystal Grwth* 2008;310:3488-97.
- [43] Krause A, Uhlemann M, Gebert A, Schultz L. The effect of magnetic fields on the electrodeposition of cobalt, *Electrochim Acta* 2004;49:4127-34.

- [44] Lee KH, Yoo J, Ko J, Kim H, Chung H, Chang D. Fabrication of biaxially textured Ni tape for YBCO coated conductor by electrodeposition, *Phys C* 2002;372:866-8.
- [45] Wang L, Gao Y, Xu T, Xue Q. A comparative study on the tribological behavior of nanocrystalline nickel and cobalt coatings correlated with grain size and phase structure, *Mat Chem Phys* 2006;99:96-103.
- [46] Kurant Z, Wawro A, Maziewski A, Maneikis A, Baczewski LT. The influence of annealing on magnetic properties of ultrathin cobalt film, *Mol Phys Rep* 2004;40:104-7.
- [47] Harada K, Tsurekawa S, Watanabe T, Palumbo G. Enhancement of homogeneity of grain boundary microstructure by magnetic annealing of electrodeposited nanocrystalline nickel, *Scr Mater* 2003;49:367-72.
- [48] Li D, Levesque A, Wang Q, Franczak A, Wu C, Chopart J-P, He J. High magnetic field annealing dependent the morphology and microstructure of nanocrystalline Co/Ni bilayered films, *CMC* 2012;30(3):207-18.
- [49] Yu M, Qiu H, Chen X. Effect of vacuum magnetic annealing on the structural and physical properties of the Ni and Al co-doped ZnO films, *Thin Solid Films* 2010;518:7174-82.
- [50] Mikelson AE, Karklin YK. Control of crystallization processes by means of magnetic fields, *J Crys Grwth* 1981;52:524-9.
- [51] Savitisky EM, Torchinova RS, Turanoy SAJ. Effect of crystallization in magnetic field on the structure and magnetic properties of Bi-Mn alloys, *J Cryst Grwth* 1981;52:519-23.
- [52] Zhao Y, Li D, Wang Q, Franczak A, Levesque A, Chopart J-P, He J. The accelerating effect of high magnetic field annealing on the interdiffusion behavior of Co/Ni films, *Mater Lett* 2013;106:190-2.
- [53] An Z, Pan S, Zhang J. Synthesis and Tunable Assembly of Spear-like Nickel Nanocrystallites: From Urchin-like Particles to Prickly Chains, *J Phys Chem C* 2009;113:1346-51.
- [54] Rudolf S. *Nanoscale Magnetic Materials and Applications*, Springer-Verlag US 2009, pp.275-307.
- [55] El Asri T, Raissi M, Vizzini S, Maachi AE, Ameziane EL, D'Avitaya FA, Lazzari JL, Coudreau C, Oughaddou H, Aufray B, Kaddouri A. Inter-diffusion of cobalt and silicon through an ultra thin aluminum oxide layer, *Appl Surf Sci* 2009;256:2731-4.
- [56] Casoli F, Nasi L, Albertini F, Fabbri S, Bocchi B, Germini F, Luches P, Rota A, Valeri S. Morphology evolution and magnetic properties improvement in FePt epitaxial films by in situ annealing after growth, *J Appl Phys* 2008;103:043912.
- [57] Guan S, Nelson BJ. Pulse-reverse electrodeposited nanograinsized CoNiP thin films and microarrays for MEMS actuators, *J Electrochem Soc* 2005;152(4):C190-5.

- [58] Homma T, Suzuki M, Osaka T. Gradient control of magnetic properties in electroless-deposited CoNiP thin films, *J Electrochem Soc* 1998;145(1):134-8.
- [59] Sun M, Zangari G, Shamsuzzoha M, Metzger RM. Electrodeposition of highly uniform magnetic nanoparticle arrays in ordered alumite, *Appl Phys Lett* 2001;78:2964-6.
- [60] Klement U, Silva MD. Thermal Stability of Electrodeposited Nanocrystalline Ni and Co-Based Materials. *Proceedings of Sino-Swedish Structural Materials Symposium* 2007.
- [61] Li YB, Lou YF, Zhang LR, Ma B, Bai JM, Wei FL. Effect of magnetic field annealing on microstructure and magnetic properties of FePt films, *J Magn Magn Mater* 2010;322:3789-91.
- [62] Shamaila S, Sharif R, Chen JY, Liu HR, Han XF. Magnetic field annealing dependent magnetic properties of $\text{Co}_{90}\text{Pt}_{10}$ nanowire arrays, *J Magn Magn Mater* 2009;321:3984-9.
- [63] Harada K, Tsurekawa S, Watanabe T, Wantanabe T, Palumbo G. Enhancement of homogeneity of grain boundary microstructure by magnetic annealing of electrodeposited nanocrystalline nickel, *Scripta Mater* 2003;49:367-72.
- [64] Zhang X, Wang D, Zhang S. Effect of high magnetic field annealing on the microstructure and magnetic properties of Co-Fe layered double hydroxide, *J Magn Magn Mater* 2010;322:3023-7.
- [65] Li D, Wang K, Wang Q, Ma X, Wu C, He J. Diffusion interaction between Al and Mg controlled by a high magnetic field, *J Appl Phys A* 2011;105:969-74.
- [66] Molodov DA, Konijnenberg PJ. Grain boundary and grain structure control through application of a high magnetic field, *Scripta Mater* 2006;54:977-81.
- [67] Watanabe T, Tsurekawa S, Zhao X, Zuo L. Grain boundary engineering by magnetic field application, *Scripta Mater* 2006;54:969-75.
- [68] Lew KS, Raja M, Thanikaikarasan S, Kim T, Kim YD, Mahalingam T. Effect of pH and current density in electrodeposited Co-Ni-P alloy thin films, *Mater Chem Phys* 2008;112:249-53.
- [69] Tian LL, Xu JC, Qiang CW. The electrodeposition behaviors and magnetic properties of Ni-Co films, *Appl Surf Sci* 2011;257:4689-94.